DichroCalc: Improvements in Computing Protein Circular Dichroism Spectroscopy in the Near-Ultraviolet

Sarah B. Jasim, Zhuo Li, Ellen E. Guest and Jonathan D. Hirst

School of Chemistry, *University of Nottingham, University Park, Nottingham NG7 2RD, United Kingdom*

Correspondence to Jonathan D. Hirst: *jonathan.hirst@nottingham.ac.uk*

https://doi.org/10.1016/j.jmb.2017.12.009

Edited by Michael Sternberg

Abstract

A fully quantitative theory connecting protein conformation and optical spectroscopy would facilitate deeper insights into biophysical and simulation studies of protein dynamics and folding. The web server DichroCalc (http://comp.chem.nottingham.ac.uk/dichrocalc) allows one to compute from first principles the electronic circular dichroism spectrum of a (modeled or experimental) protein structure or ensemble of structures. The regular, repeating, chiral nature of secondary structure elements leads to intense bands in the far-ultraviolet (UV). The near-UV bands are much weaker and have been challenging to compute theoretically. We report some advances in the accuracy of calculations in the near-UV, realized through the consideration of the vibrational structure of the electronic transitions of aromatic side chains. The improvements have been assessed over a set of diverse proteins. We illustrate them using bovine pancreatic trypsin inhibitor and present a new, detailed analysis of the interactions which are most important in determining the near-UV circular dichroism spectrum.

Introduction

Circular dichroism (CD) in the near-ultraviolet (near-UV) is widely used to study structural changes in proteins, because of its sensitivity [1,2] to, for example, ligand binding, changes of the environment and catalysis [3]. The hydrophobic packing of aromatic side chains of amino acids is a key determinant of structure of proteins [4]. Aromatic side chains are often found in enzyme active sites, where they play an important role in molecular recognition and biological function. Thus, biospectroscopic investigations of aromatic–aromatic interactions can provide new information on protein structure and dynamics. The local conformation of the protein chain around an aromatic ring influences the $\pi\pi^*$ electronic excitations of phenylalanine, tyrosine, and tryptophan, and the coupling of the various excitations is sensitive to the relative orientation and proximity of the aromatic groups.

CD is the differential absorption of left-handed and right-handed circularly polarized light. Bands in CD spectra in the near-UV occur between 240 and 300 nm. They provide useful information on the environment and interactions of aromatic side chains and the measurement of near-UV CD of proteins has been instrumental, for example, in characterizing intermediates in the folding process [5]. A combination of CD measurement and computational approaches (if sufficiently accurate) can offer a powerful means of investigating the conformations of large biopolymers.

Methods for computing the CD of proteins from first principles are well established. The background and methodology has been reviewed elsewhere [6]. These techniques are necessarily more approximate than fully quantum mechanical methods, such as time-dependent density functional theory, which are only tractable at the moment on systems of the size of small peptides [7]. A central component of approximate approaches for computing protein CD is the set of parameters used to model the electronic excitations of the various chromophores in proteins. Over the years, we have used *ab initio* quantum chemical methods to develop parameter sets that have improved the accuracy of protein CD

Please cite this article as: S. B. Jasim, et al., DichroCalc: Improvements in Computing Protein Circular Dichroism Spectroscopy in the Near-Ultraviolet, J. Mol. Biol. (2018), https://doi.org/10.1016/j.jmb.2017.12.009

calculations, in the vacuum-UV [8], where bands arise due to charge-transfer transitions, in the far-UV [9], where the backbone $n\pi^*$ and $\pi\pi^*$ transitions appear, and in the near-UV [10,11], where the main contribution is from the aromatic L_a and L_b $\pi\pi^*$ transitions. These parameters and the computational methodology are available via our DichroCalc web interface [12] and have been used by over 1400 different researchers to compute the CD spectra of more than 3.3 million structures, including all the proteins in the Protein Data Bank (PDB) [13], models and snapshots from molecular dynamics (MD) simulations. Software implementing analogous methodology to that in DichroCalc has recently been made available, for example, ProtPol [14], but the DichroCalc web interface makes the computational methodology, including some unique theoretical aspects, accessible to a wider community.

The focus of this paper is on new developments. First, however, we give a few illustrative examples of some of the applications of DichroCalc. In contrast to the analysis of protein CD spectra to extract information (perhaps on secondary structure content) through the application of statistical or machine learning methods, which is an active field in its own right [15,16], the focus of DichroCalc and its applications usually start with the generation of atomistic models (or hypotheses) of structure and/or conformational change, followed by computation, from first principles, of the CD spectra that would be predicted to arise. DichroCalc has been used [17] to compute the CD spectra of amyloid structures, based on MD simulations. Calculated CD spectra have also been used in the comparison of simulated conformations of Mets7, bound and unbound to cis-platin [18]; Mets7 is an eight-residue peptide, which mimics an important function, that is, cellular uptake of platinum-based drugs, of the high-affinity copper influx transporter protein, Ctr1. Simulations of a phosphate binding protein labeled with two rhodamine fluorophores have been conducted [19], because the protein was not amenable to study by X-ray crystallography or NMR spectroscopy; comparison with experimental biophysical data was facilitated by computing the CD from the MD simulations. A similar approach has been adopted to help design mutants of the coiled-coil domain of the oncoprotein Bcl–Abl [20]; vacuum-UV CD spectrum of human myelin P2 protein has been computed [21] using DichroCalc and qualitatively agreed with experimental measurements made using synchrotron radiation. Simulations and DichroCalc have been used to predict the loss of helicity for peptides binding to the surface of silica [22]. As is evident from the preceding selected examples, DichroCalc is finding utility across a range of challenging problems.

There have been many biochemical and biophysical studies utilizing near-UV CD spectroscopy. The contribution of aromatic residues to the near-UV spectra has been investigated using site-directed mutagenesis [23,24]. Recently, there has been additional interest in the near-UV spectroscopy of proteins, with the advent of two-dimensional electronic spectroscopy, realizable through ultrafast laser spectroscopy, which has been used, for example, to study tryptophan-to-heme electron transfer and excitation energy transfer in myoglobin [25]. Several theoretical studies [26–28] have investigated the distinctive signatures that amyloid fibrils show in the near-UV as well as those of other proteins [29]. MD simulation and calculations of two-dimensional near-UV spectroscopy have been used to monitor the unfolding of a tetrapeptide after photo-induced reduction of an internal disulfide bond [30].

In contrast to intense bands in the far-UV, near-UV bands are much weaker and have been challenging to compute theoretically. We have recently [11] made some advances in the accuracy of calculations in the near-UV, realized through the consideration of the vibrational structure of the electronic transitions of aromatic side chains and significant improvements have been established over a set of diverse proteins. The conformational influences of protein structure on near-UV CD spectra are rooted in the same fundamental physical origins as those on the far-UV CD spectra, but the structural relationship is most likely rather more subtle than in the far-UV, where the regular, repeating nature of the backbone chain in well-defined secondary structures dominates. Herein, we investigate these origins, using our new parameters for the aromatic chromophores.

The intensity or rotational strength of a transition in a CD spectrum may arise from three mechanisms coupling electronic transitions. The *one-electron mechanism* [31] involves two transitions within the same chromophore and is also known as intra-chromophore mixing. The *μ–μ mechanism* is the coupling mediated by electric transition dipole moments of two separate chromophores. The *μ–m mechanism* is the coupling between the electric and magnetic transition moments of two separate chromophores [32]. Several studies have investigated the role of these mechanisms in determining the nature of the near-UV CD spectra of the proteins TEM-1 β-lactamase [33–37] and human carbonic anhydrase [38].

We have recently updated and enhanced the DichroCalc web server with new models of the aromatic side-chain chromophores, which incorporate the vibrational structure within the electronic bands in the near-UV. The near-UV CD spectra of 40 proteins computed with the new parameter set agree well with experiment and much better than spectra calculated with previous parameters [10,39]. Accounting for conformational flexibility by using families of NMR structures, instead of the X-ray structure, improved the calculated spectrum for several proteins. This

Please cite this article as: S. B. Jasim, et al., DichroCalc: Improvements in Computing Protein Circular Dichroism Spectroscopy in the Near-Ultraviolet, J. Mol. Biol. (2018), https://doi.org/10.1016/j.jmb.2017.12.009

suggested an informative level of sensitivity to side-chain conformation and provides a means for us to examine the detailed influences of structure on the spectrum. In what follows, we investigate the contributions to the near-UV CD spectra computed for a family of NMR structures for bovine pancreatic trypsin inhibitor (BPTI), a protein comprising 58 residues, including four phenylalanines (Phe4, Phe22, Phe33, Phe45), four tyrosines (Tyr10, Tyr21, Tyr23, Tyr35) and three disulfide bonds.

Results and Discussion

The quality of the calculated near-UV CD spectra has been systematically assessed [11] over a set of 40 proteins, for which there are published experimental spectra. The correlation between the computed and the experimental intensity from 270 to 290 nm is much improved; the root mean squared error (RMSE) in the computed intensity in this wavelength range is reduced by typically a factor of two compared to the previous best calculations. The calculations do not yet give a fully quantitative agreement with experiment. However, in addition to the significant improvement in statistical measures such as RMSE, mean relative error and correlation, there is a striking qualitative improvement which arises from reproduction of the vibrational features clearly evident in the near-UV spectra.

The near-UV CD spectra of BPTI calculated using the X-ray crystal structure form II (PDB code: 5PTI; the structure is shown Fig. S1 of the Supplemental Information) and separately an average over the 20 NMR structures (PDB code: 1PIT) are compared to the experimental spectrum [40] in Fig. 1. The X-ray crystal structure leads to a computed spectrum that reproduces the overall shape and location of the peaks reasonably well, but the intensity across the wavelength range is noticeably underestimated. The spectrum calculated by averaging over the NMR structures is about 20% more intense and the RMSE with respect to the experimental spectrum is correspondingly reduced (from 128 to 91 deg cm^2 $dmol^{-1}$). The conformational diversity of BPTI in solution is reflected, at least in part, by the family of NMR structures. Figure 1 shows the CD spectrum calculated using specific NMR structures: frame 3 and frame 5, which give the more intense spectra (in closest agreement with experiment), and by way of contrast frame 17, which gives the calculated spectrum of weakest intensity. The structural difference across these three frames is small, varying from 0.8 to 1.1 Å all-atom RMSD.

The spectrum computed from averaging over all the NMR frames is less intense than the experimental spectrum. However, two particular NMR frames, 3 and 5, lead to computed spectra in excellent agreement (both with an RMSE of 49 deg cm^2 $dmol^{-1}$) with

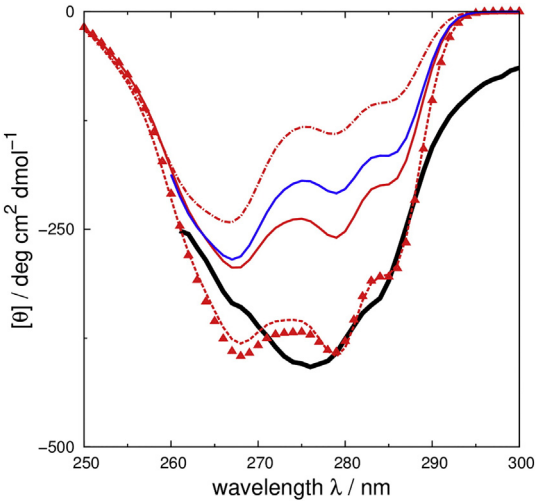

Fig. 1. Experimental [40] near-UV CD spectrum (black solid line), and spectra calculated using the X-ray structure (blue solid line), calculated using an average over 20 frames of the NMR structure (red solid line) and calculated from individual frames of the NMR structure: frame 3 (dashed red line with triangles), frame 5 (dotted red line) and frame 17 (red dot-dashed line).

experiment. The contributions of the phenylalanine and tyrosine chromophores are clearly well reproduced. The good agreement and the sensitivity to modest structural differences motivate us to investigate the detailed interactions that govern the spectrum.

The interactions of different transitions in the protein environment are computed in the exciton matrix method calculation as the purely electrostatic, Coulombic interaction energy between two transition charge densities, each represented by a set of point charges (as part of the parameter set, described in detail in our earlier work [11]). They depend on the charge densities and on their relative orientation and separation. In the case of the one-electron mechanism, there is a dependence on the surrounding ground state electronic density. The significant interaction energies (i.e., those greater than 1 cm^{-1}) for frame 3 are shown in Table 1. Coupling between L states and B states (the latter occurring in the far-UV) is weak. The largest interaction energy is 84.9 cm^{-1} and corresponds to the one-electron mixing of the $^1L_{b,\,v2}$ and ^1L_a transitions of Tyr23 (*v2* denotes that the transition is to the second vibrational level of the excited state). The analogous transitions on Tyr10 interact via the same mechanism and with a very similar magnitude. Inter-chromophore interactions are much weaker, and with the exception of the interaction between Phe22 and Phe33 (27.4 cm^{-1}), they are all less than 10 cm^{-1}; for example, the interaction between Phe22 $^1L_{b,v1}$ and Phe45 ^1L_a is −1.4 cm^{-1}. The interaction energies for frame 5 have a very similar pattern (data not shown).

Please cite this article as: S. B. Jasim, et al., DichroCalc: Improvements in Computing Protein Circular Dichroism Spectroscopy in the Near-Ultraviolet, J. Mol. Biol. (2018), https://doi.org/10.1016/j.jmb.2017.12.009

Table 1. Calculated interaction energies (shown only if greater than 1 cm^{-1}) of the electronic transitions of aromatic side chains in frame 3 of the NMR structure of BPTI (PDB code: 1PIT)

Chromophore/ Transition[a]	Chromophore/ Transition[a]	Separation (Å)	Interaction energy (cm^{-1})
Phe4 ^1L_b *v*1	Phe45 ^1L_b *v*1	9.6	1.3
Phe22 ^1L_b *v*1	Phe33 ^1L_a	5.2	27.4
Phe22 ^1L_b *v*1	Phe45 ^1L_a	7.8	−1.4
Phe22 ^1L_a *v*1	Tyr23 ^1L_b *v*2	9.8	−1.2
Phe33 ^1L_b *v*1	Tyr21 ^1L_a	8.8	1.9
Phe33 ^1L_a	Tyr35 ^1L_b *v*2	8.9	−5.4
Phe45 ^1L_b *v*1	Tyr21 ^1L_a	8.6	3.5
Tyr10 ^1L_b *v*2	Tyr10 ^1L_a	0.0[b]	80.9
Tyr10 ^1L_a	Tyr35 ^1L_b *v*2	8.9	2.8
Tyr21 ^1L_b *v*2	Tyr35 ^1L_a	13.5	1.6
Tyr23 ^1L_b *v*2	Tyr23 ^1L_a	0.0	84.9
Tyr23 ^1L_a	Tyr35 ^1L_a	19.8	1.6
Tyr35 ^1L_b *v*2	Tyr35 ^1L_a	0.0	6.7

[a] Vibrational levels of ^1L_b states are denoted *v*1 or *v*2; only these levels showed significant interactions.
[b] A separation of 0 Å corresponds to the one-electron mixing of two transitions on the same chromophore.

From the interaction energies in Table 1, it is clear that the one-electron mixing of the tyrosine ^1L_b states is an important factor in the appearance of the near-UV spectrum. This is confirmed by a detailed examination of the intensity (i.e., rotational strength) of each transition in the calculated spectrum. The most intense transitions in this region arise from the tyrosine residues (Table 2), with the phenylalanine transitions making a more modest contribution (Table S1 of the Supplemental Information); the electric and magnetic transition dipole moments of the phenylalanine residues are substantially smaller than those for the tyrosine residues. The data in Table 2 are computed using frame 3 of the NMR structure; frame 5 gives similar values, whereas for frame 17, the values are significantly smaller (Table S2 of the Supplemental Information). The limited interaction between transitions on different chromophores makes it straightforward to assign transitions in the calculated spectrum to specific transitions on specific residues. In the absence of any chirality, the electric and magnetic transition dipole moments of an excitation would be perpendicular, and the rotational strength, which is directly proportional to the dot product of these two vectors would be zero. Even small deviations from perpendicularity give rise to a non-zero intensity. Table 2 shows for each tyrosine ^1L_b transition the contribution of the angle between the electric and magnetic transition dipole moments to the intensity. An angle less than 90° would lead to a positive intensity; an angle greater than 90° gives a negative rotational strength. The angles in Table 2 exhibit some variation and a delicate balance (of positive and negative contributions) across the transitions is responsible for the overall intensity. The predominance of the one-electron mechanism in the near-UV CD of BPTI leads to significant sensitivity of the spectrum to the precise nature of the local environment surrounding the tyrosine residues.

The above exemplar, taken from a wide range of proteins used to benchmark our latest calculations, demonstrates that a significant advance in quantitative modeling of the near-UV CD spectra of proteins has been achieved through more sophisticated modeling of the electronic and vibronic structure of the relevant chromophores. The conformational dynamics, as reflected in the calculations using a family of NMR structures compared to an X-ray crystal structure, and the influence of the local electrostatic environment are other factors that can also be important. The latter aspect, in particular, will be a focus for future development, along with the development of parameters for the disulfide bond

Table 2. The eight (*v* = 1 to 8) tyrosine ^1L_b vibrational states, their wavelengths (λ) and their calculated contributions to the rotational strength (in Debye Bohr magneton) at that wavelength (R_λ) in the near-UV CD spectrum of BPTI (computed for frame 3 of the NMR structure)

v	λ (nm)	Tyr35[a] μm[b]	cosθ[c]	Tyr21 μm	cosθ	Tyr10 μm	cosθ	Tyr23 μm	cosθ	R_λ/DBM × 1000[d]
1	286.1	0.52	0.03	0.31	−0.06	0.45	−0.05	0.39	−0.01	−29
2	279.7	0.64	0.02	0.39	−0.05	0.59	−0.05	0.51	−0.01	−34
3	276.1	0.05	0.03	0.01	−0.47	0.02	−0.06	0.01	−0.09	−8
4	273.5	0.36	0.02	0.21	−0.07	0.33	−0.05	0.29	−0.01	−25
5	270.2	0.05	0.02	0.01	−0.42	0.03	−0.07	0.02	−0.07	−9
6	267.6	0.13	0.01	0.06	−0.16	0.11	−0.05	0.09	−0.02	−16
7	264.5	0.04	0.00	0.01	−0.37	0.01	−0.09	0.01	−0.19	−7
8	262.0	0.04	−0.01	0.01	−0.36	0.01	−0.09	0.01	−0.19	−7

[a] BPTI has four tyrosines; thus, there are four contributions at each wavelength.
[b] The μm value given in the table is not the scalar product, but simply the product of the magnitudes of the electric and magnetic transition dipole moments.
[c] In an achiral environment, the electric and magnetic transition dipole moments would be perpendicular (cosθ = 0).
[d] The rotational strength, $R = \mu m \cos\theta$, where μ is the magnitude of the electric transition dipole moment, m is the magnitude of the magnetic transition dipole moment and θ is the angle between them.

Please cite this article as: S. B. Jasim, et al., DichroCalc: Improvements in Computing Protein Circular Dichroism Spectroscopy in the Near-Ultraviolet, J. Mol. Biol. (2018), https://doi.org/10.1016/j.jmb.2017.12.009

(which has not been considered in the current work). The more quantitative nature of the near-UV CD calculations should help molecular simulation studies of protein structure and dynamics make more direct connections with both equilibrium and time-resolved experiments, and potentially could provide additional useful information for NMR structure determination. There are, of course, many other molecules that form interesting chiral macromolecular structures and that contain aromatic chromophores; a couple of examples which we have studied previously include oligoureas [41] and naphthalenediimide nanotubes [42]. Thus, calculations of near-UV CD spectra, using our web server DichroCalc, will find applicability across many types of macromolecular system.

Materials and Methods

We took the coordinates of BPTI from the X-ray crystal structure (PDB code: 5PTI) and from the NMR models (PDB code: 1PIT). The theoretical framework, an exciton approach [43] or the so-called matrix method [44,45], embodied in DichroCalc has been described fully elsewhere [6,9]. Recently, we have described the extension of the approach to include vibrational structure in the far-UV [46]. Vibrational structure is an important, but not the sole, contributor to the bandwidth of transitions. Extension of the approach is exactly analogous for the near-UV [11], where we have developed new parameters for the phenylalanine (Phe), tyrosine (Tyr) and tryptophan (Trp) side chains, each of which has four electronic states (L_b, L_a, B_b, B_a) as labeled by Platt [47]. For near-UV CD spectra, the main focus of interest is the L_b and L_a transitions; the higher-energy B_b and B_a transitions occur in the far-UV [48]. For phenylalanine and tyrosine, the vibrational structure of only the ^1L_b excited states was considered, since their ^1L_a states are located at higher energies. Toluene is used to represent the aromatic side chain of phenylalanine and *p*-cresol is used to represent tyrosine. The vibrational transitions are included by extending the exciton Hamiltonian [11] and modifying by scaling (by a normalized Franck–Condon overlap integral) the electric transition dipole moments and the monopole charges representing the transition charge densities. Interactions between the vibrational levels of the same chromophore are not considered. We include the first six to nine transitions in a vibrational progression. The new parameters can be accessed via the DichroCalc web interface. Transitions of the peptide backbone ($n\pi^*$ and $\pi\pi^*$) [9] and the B_a, B_b and L_a transitions of the aromatic side chains were included in the calculation, but no vibrational structure is considered for these transitions. The calculations yield a set of rotational strengths and corresponding transition energies, initially in the form of line spectra, which, to facilitate comparison with experimental spectra, are convolved with Gaussian bands. In this study, for the near-UV region, we have used a Gaussian function with a bandwidth of 4 nm.

Acknowledgments

This work was supported by the Engineering and Physical Sciences Research Council [grant numbers EP/P020232/1, EP/R512059/1]; the Iraqi Ministry of Higher Education and Scientific Research; and a University of Nottingham Vice-Chancellor's scholarship. We are grateful for access to the University of Nottingham High Performance Computing facility, and to the HPC Midlands Plus Tier-2 Centre. DichroCalc is freely available for use via http://comp.chem.nottingham.ac.uk.

Appendix A. Supplementary data

Supplementary data to this article can be found online at https://doi.org/10.1016/j.jmb.2017.12.009.

Received 25 October 2017;
Received in revised form 24 November 2017;
Accepted 10 December 2017
Available online xxxx

Keywords:
aromatic;
vibronic;
ab initio;
electronic excited states;
quantum

Abbreviations used:
BPTI, bovine pancreatic trypsin inhibitor; CD, circular dichroism; MD, molecular dynamics; PDB, Protein Data Bank.

References

[1] R.W. Woody, A.K. Dunker, in: G.D. Fasman (Ed.), Circular Dichroism and the Conformational Analysis of Biomolecules, Plenum Press, New York, 1996.
[2] S.M. Kelly, T.J. Jess, N.C. Price, How to study proteins by circular dichroism, Biochim. Biophys. Acta Protein Proteomics 1751 (2005) 119–139.
[3] P.C. Kahn, The interpretation of near-ultraviolet circular dichroism, Methods Enzymol. 61 (1979) 339–378.
[4] S.K. Burley, G.A. Petsko, Aromatic–aromatic interaction—a mechanism of protein-structure stabilization, Science 229 (1985) 23–28.
[5] O.B. Ptitsyn, Molten globule and protein folding, Adv. Protein Chem. 47 (1995) 83–229.

[6] B.M. Bulheller, A. Rodger, J.D. Hirst, Circular and linear dichroism of proteins, Phys. Chem. Chem. Phys. 9 (2007) 2020–2035.
[7] J. Kaminsky, J. Kubelka, P. Bour, Theoretical modeling of peptide alpha-helical circular dichroism in aqueous solution, J. Phys. Chem. A 115 (2011) 1734–1742.
[8] B.M. Bulheller, A.J. Miles, B.A. Wallace, J.D. Hirst, Charge-transfer transitions in the vacuum-ultraviolet of protein circular dichroism spectra, J. Phys. Chem. B 112 (2008) 1866–1874.
[9] N.A. Besley, J.D. Hirst, Theoretical studies toward quantitative protein circular dichroism calculations, J. Am. Chem. Soc. 121 (1999) 9636–9644.
[10] D.M. Rogers, J.D. Hirst, First-principles calculations of protein circular dichroism in the near ultraviolet, Biochemistry 43 (2004) 11092–11102.
[11] Z. Li, J.D. Hirst, Quantitative first principles calculations of protein circular dichroism in the near-ultraviolet, Chem. Sci. 8 (2017) 4318–4333.
[12] B.M. Bulheller, J.D. Hirst, DichroCalc-circular and linear dichroism online, Bioinformatics 25 (2009) 539–540.
[13] C. Louis-Jeune, M.A. Andrade-Navarro, C. Perez-Iratxeta, Prediction of protein secondary structure from circular dichroism using theoretically derived spectra, Proteins: Struct. Funct. Bioinf. 80 (2012) 374–381.
[14] K. Matsuo, H. Hiramatsu, K. Gekko, H. Namatame, M. Taniguchi, R.W. Woody, Characterization of intermolecular structure of beta(2)-microglobulin core fragments in amyloid fibrils by vacuum-ultraviolet circular dichroism spectroscopy and circular dichroism theory, J. Phys. Chem. B 118 (2014) 2785–2795.
[15] V. Hall, A. Nash, E. Hines, A. Rodger, Elucidating protein secondary structure with circular dichroism and a neural network, J. Comput. Chem. 34 (2013) 2774–2786.
[16] A. Micsonai, F. Wien, L. Kernya, Y.-H. Lee, Y. Goto, M. Réfrégiers, J. Kardos, Accurate secondary structure prediction and fold recognition for circular dichroism spectroscopy, Proc. Natl. Acad. Sci. U. S. A. 112 (2015) E3095–E3103.
[17] I.W. Hamley, D.R. Nutt, G.D. Brown, J.F. Miravet, B. Escuder, F. Rodriguez-Llansola, Influence of the solvent on the self-assembly of a modified amyloid beta peptide fragment. II. NMR and computer simulation investigation, J. Phys. Chem. B 114 (2010) 940–951.
[18] T.H. Nguyen, F. Arnesano, S. Scintilla, G. Rossetti, E. Ippoliti, P. Carloni, G. Natile, Structural determinants of cisplatin and transplatin binding to the Met-rich motif of Ctr1: a computational spectroscopy approach, J. Chem. Theory Comput. 8 (2012) 2912–2920.
[19] M.B. Goncalves, J. Dreyer, P. Lupieri, C. Barrera-Patino, E. Ippoliti, M.R. Webb, J.E.T. Corrie, P. Carloni, Structural prediction of a rhodamine-based biosensor and comparison with biophysical data, Phys. Chem. Chem. Phys. 15 (2013) 2177–2183.
[20] A.S. Dixon, S.S. Pendley, B.J. Bruno, D.W. Woessner, A.A. Shimpi, T.E. Cheatham, C.S. Lim, Disruption of Bcr–Abl coiled coil oligomerization by design, J. Biol. Chem. 286 (2011) 27,751–27,760.
[21] V. Majava, E. Polverini, A. Mazzini, R. Nanekar, W. Knoll, J. Peters, F. Natali, P. Baumgartel, I. Kursula, P. Kursula, Structural and functional characterization of human peripheral nervous system myelin protein P2, PLoS One 5 (2010), e10300.
[22] R.H. Meissner, J. Schneider, P. Schiffels, L.C. Ciacchi, Computational prediction of circular dichroism spectra and quantification of helicity loss upon peptide adsorption on silica, Langmuir 30 (2014) 3487–3494.
[23] P.O. Freskgard, L.G. Martensson, P. Jonasson, B.H. Jonsson, U. Carlsson, Assignment of the contribution of the tryptophan residues to the circular-dichroism spectrum of human carbonic-anhydrase II, Biochemistry 33 (1994) 14281–14288.
[24] A.Y.M. Woody, R.W. Woody, Individual tyrosine side-chain contributions to circular dichroism of ribonuclease, Biopolymers 72 (2003) 500–513.
[25] C. Consani, G. Aubock, F. van Mourik, M. Chergui, Ultrafast tryptophan-to-heme electron transfer in myoglobins revealed by UV 2D spectroscopy, Science 339 (2013) 1586–1589.
[26] J. Jiang, D. Abramavicius, C. Falvo, B.M. Bulheller, J.D. Hirst, S. Mukamel, Simulation of two-dimensional ultraviolet spectroscopy of amyloid fibrils, J. Phys. Chem. B 114 (2010) 12,150–12,156.
[27] A.R. Lam, J. Jiang, S. Mukamel, Distinguishing amyloid fibril structures in Alzheimer's disease (AD) by two-dimensional ultraviolet (2DUV) spectroscopy, Biochemistry 50 (2011) 9809–9816.
[28] A.R. Lam, J.J. Rodriguez, A. Rojas, H.A. Scheraga, S. Mukamel, Tracking the mechanism of fibril assembly by simulated two-dimensional ultraviolet spectroscopy, J. Phys. Chem. A 117 (2013) 342–350.
[29] J. Li, M.S. Deng, D.V. Voronine, S. Mukamel, J. Jiang, Two-dimensional near ultraviolet (2DNUV) spectroscopic probe of structural-dependent exciton dynamics in a protein, J. Phys. Chem. B 119 (2015) 1314–1322.
[30] A. Nenov, S.A. Beccara, I. Rivalta, G. Cerullo, S. Mukamel, M. Garavelli, Tracking conformational dynamics of polypeptides by nonlinear electronic spectroscopy of aromatic residues: a first-principles simulation study, ChemPhysChem 15 (2014) 3282–3290.
[31] E.U. Condon, W. Alter, H. Eyring, One-electron rotatory power, J. Chem. Phys. 5 (1937) 753–775.
[32] J.A. Schellman, Symmetry rules for optical rotation, Acc. Chem. Res. 1 (1986) 144–151.
[33] C. Christov, T. Karabencheva, Mechanisms of generation of rotational strengths in TEM-1 β-lactamase. Part I: theoretical analysis of the influence of conformational changes in the near-UV, Chem. Phys. Lett. 396 (2004) 282–287.
[34] C.Z. Christov, T.G. Karabencheva, A. Lodola, Relationship between chiroptical properties, structural changes and interactions in enzymes: a computational study on β-lactamases from class A, Comput. Biol. Chem. 32 (2008) 167–175.
[35] C.Z. Christov, T.G. Karabencheva, A. Lodola, Aromatic interactions and rotational strengths within protein environment: an electronic structural study on β-lactamases from class A, Chem. Phys. Lett. 456 (2008) 89–95.
[36] T.G. Karabencheva, R. Donev, K. Balali-Mood, C.Z. Christov, Individual contributions of the aromatic chromophores to the near-UV circular dichroism in class A β-lactamases: a comparative computational analysis, Biophys. Chem. 151 (2010) 39–45.
[37] C.Z. Christov, T.G. Karabencheva, Computational insight into protein circular dichroism: detailed analysis of contributions of individual chromophores in TEM-1 β-lactamase, Theor. Chem. Accounts 128 (2011) 25–37.
[38] T.G. Karabencheva-Christova, U. Carlsson, K. Balali-Mood, G.W. Black, C.Z. Christov, Conformational effects on the circular dichroism of human carbonic anhydrase II: a multilevel computational study, PLoS One 8 (2013), e56874.

Please cite this article as: S. B. Jasim, et al., DichroCalc: Improvements in Computing Protein Circular Dichroism Spectroscopy in the Near-Ultraviolet, J. Mol. Biol. (2018), https://doi.org/10.1016/j.jmb.2017.12.009

[39] D.M. Rogers, J.D. Hirst, Ab initio study of aromatic side chains of amino acids in gas phase and solution, J. Phys. Chem. A 107 (2003) 11,191–11,200.
[40] N. Sreerama, M.C. Manning, M.E. Powers, J.X. Zhang, D.P. Goldenberg, R.W. Woody, Tyrosine, phenylalanine, and disulfide contributions to the circular dichroism of proteins: circular dichroism spectra of wild-type and mutant bovine pancreatic trypsin inhibitor, Biochemistry 38 (1999) 10,814–10,822.
[41] M.T. Oakley, G. Guichard, J.D. Hirst, Calculations on the electronic excited states of ureas and oligoureas, J. Phys. Chem. B 111 (2007) 3274–3279.
[42] B.M. Bulheller, G.D. Pantos, J.K.M. Sanders, J.D. Hirst, Electronic structure and circular dichroism spectroscopy of naphthalenediimide nanotubes, Phys. Chem. Chem. Phys. 11 (2009) 6060–6065.
[43] A. Davydov, Theory of Molecular Excitons, Plenum Press, New York, 1971.
[44] P.M. Bayley, E.B. Nielsen, J.A. Schellman, Rotatory properties of molecules containing two peptide groups: theory, J. Phys. Chem. 73 (1969) 228–243.
[45] R.W. Woody, I. Tinoco, Optical rotation of oriented helices. III. Calculation of the rotatory dispersion and circular dichroism of the alpha-and 310-helix, J. Chem. Phys. 46 (1967) 4927–4945.
[46] Z. Li, D. Robinson, J.D. Hirst, Vibronic structure in the far-UV electronic circular dichroism spectra of proteins, Faraday Discuss. 177 (2015) 329–344.
[47] J.R. Platt, Classification of spectra of cata-condensed hydrocarbons, J. Chem. Phys. 17 (1949) 484–495.
[48] R.W. Woody, Aromatic side-chain contributions to protein circular dichro ism, in: V.N. Uversky, E.A. Permyakov (Eds.), Methods in Protein Structure and Stability Analysis, Nova Science Publishers, 2007.

Please cite this article as: S. B. Jasim, et al., DichroCalc: Improvements in Computing Protein Circular Dichroism Spectroscopy in the Near-Ultraviolet, J. Mol. Biol. (2018), https://doi.org/10.1016/j.jmb.2017.12.009